Contribution

Structural Characteristic of Iron(III) Chelates to Induce Tissue Damage and Renal Carcinoma; Chemical Origin of the Iron Toxicity

Yuzo Nishida*

Yamagata University
1-4-12 Kojirakawa-machi, Yamagata-shi, 990-8560 Japan

1. Introduction

It is generally recognized that iron, the most abundant transition metal ion in mammalian systems, is a necessary trace element and is required for normal metabolic processes spanning molecular oxygen transport, respiratory electron transfer, DNA synthesis, and drug metabolism.[1,2] In fact, iron deficiency leads to the deficiency of neurotransmitters such as dopamine and serotonin in brain, inducing several mental diseases such as Parkinson's disease, depression and schizophrenia, *etc.*[3] Thus, the ancient Greeks concocted potions of iron filings dissolved in vinegar, hoping that drinking this liquor would empower them with the properties of the element.[1]

After this recognition as an essential nutrient, the common assumption (but this has become apparent to be incorrect based on recent research) was made that "more is better". This assumption persists today. Health professionals have been no more exempt from this line of reasoning than the rest of society. Accordingly, for several decades we have sold the idea that "iron-fortified" foods will make us healthier and stronger, when in truth, this holds only for the persons who are frankly iron deficient. For the majority of persons, iron supplementation simply results in ever-increasing store of excess iron in the body.

In the human body, we have no real mechanism for the elimination of excess iron, and as a result, cells continuously store excess absorbed iron in a complex with the protein ferritin. Normal cells store iron mainly in ferritin molecules,[4,5] but under conditions of iron excess some of it is shunted into another storage form known as hemosiderin, in which the excess iron is deposited as ferrihydrate structures, containing mainly $Fe(OH)_3$. Hemosiderin is typically insoluble, and several experimental data support the hypothesis that hemosiderin is a degradation product of ferritin.

Plasma iron is normally bound to the iron transport protein transferrin. When some chelates (amino acids derivatives or small peptides) are present in the plasma, the precipitated ferrihydrate (mainly $Fe(OH)_3$) in hemosiderin may dissolve; these iron ions not associated with transferrin are generally termed as non-transferrin-bound iron (NTBI). NTBI is detected in the plasma of patients with thalassemia, hemochromatosis and other iron-overloading disorders, as well as in patients receiving chemotherapy where there is a temporary shutdown of the bone marrow and reduction in demand for transferrin-bound iron.[6-10] It should be noted here that NTBI has been thought to play an important role in iron induced cell damage with resultant peroxidation of cell membrane lipids and other biomolecules, and such oxidative damage is implicated as an important contributor in the pathogenesis of cancer, cardiovascular disease, aging and other degenerative diseases, but little is understood about the chemical composition of NTBI and the origin of toxicity due to NTBI at present.

In addition to the cellular acquisition of iron by the classic transferrin-dependent pathway, uptake of non-transferrin-bound iron (NTBI) is well documented.[11] NTBI is typically present at concentrations up to 10 µM. The abnormal distribution of tissue iron in advanced iron overload is likely to reflect the pattern of receptor-mediated NTBI uptake into different tissues such as the heart, endocrine glands, anterior pituitary and the liver. NTBI uptake may be particularly relevant in the face of iron-overload diseases such as hereditary hemochromatosis, hypotransferrinemia, and thalassemia, in which plasma iron presents in excess of transferrin-binding capacity. Under such conditions, NTBI uptake by tissues (e.g., liver, heart, and pancreas, but not brain) may serve to clear potentially toxic levels of iron from the plasma before damage due to iron-catalyzed oxygen radicals can accumulate. However, this should contribute to the pathophysiology of iron overload disorders.

Despite numerous studies over the last 30 years since plasma NTBI was first postulated to exist, it is still poorly characterized. A proportion of NTBI in iron-overloaded plasmas may exist as iron citrate complexes that are able to bind albumin as described above. The inability thus far to characterize NTBI most likely reflects both its heterogeneous nature and the likelihood that the different forms will vary with the disease state. One of the consequences of the anticipated heterogeneity is that various forms of NTBI are likely to be accessed at different rates by the iron chelators available for clinical use in the treatment of iron-overload disorders.

In this review, we will demonstrate several chemical models for NTBI, and show the chemical origin of iron toxicity in human body due to NTBI, and propose a new technique to eliminate the NTBI safely.

*Present address: Medical Research Institute, Kanazawa Medical University, 1-1 Daigaku, Uchinada, Kahoku, Ishikawa, 920-0261 Japan.

2. Iron(III)-nta Chelate as a Renal Carcinogen

Ferric nitrilotriacetate [Fe(III)-nta] is a well-known renal carcinogen, and Fe(III)-nta-injected animals have been used as a model of carcinogenesis.[11-14] When Fe(III)-nta is intraperitoneally injected into animals, lipid peroxidation and oxidative modification of proteins and DNA occur in renal proximal tubules, and tubular epithelial cells are damaged. Thiobarbituric acid reactive substances (TBARS[15]; these include malondialdehyde and other aldehyde derivatives, see Scheme 1) have also been shown to increase in kidneys, and cold Schiff staining showed lipid peroxidation in renal proximal tubules in Fe(III)-nta-treated animals. Increases in 4-hydroxy-2-nonenal (4-HNE)-modified proteins and 8-hydroxy-deoxyguanosine (8-OH-dG) were also demonstrated using biochemical and immunohistochemical methods. In Fe(III)-nta-injected mice, the amount of reduced glutathione decreased, and the oxidixed form increases when the metabolic rate of glutathione was accelerated. Repeated injections with Fe(III)-nta result in appearance of atypical epithelial cells in renal tubules, and finally in induction of renal carcinoma. Kawabata *et al.* reported that some damaged tubular cells disappeared from the tubules due to apoptosis in Fe(III)-nta injected mice.[16] In addition, Hiroyasu *et al.* reported specific allelic loss of p16 tumor suppressor gene in rats after a few weeks of repeated Fe(III)-nta injections.

From all these studies, there is no doubt that Fe(III)-nta induces renal carcinoma, but a detailed molecular mechanism of Fe(III)-nta induced carcinogenesis, and the chemical properties necessary for renal tubular injury and carcinogenesis, remain unknown at present. In order to answer the above questions, which at the same time will contribute to clarify the chemical composition of NTBI and the origin of the toxicity due to NTBI, we have continued to study the chemical mechanism of renal injury and carcinogenesis by many iron(III) chelates analogous to (nta),[17] as described in Figure 1.

We have found that the proximal tubules necrosis induced by artificial iron(III)-chelates in rat kidneys is highly dependent on the chelate structure (see Table 1), and injuries such as lipid peroxidation and protein oxidation are observed mainly in the renal proximal tubules, but injuries were not observed in the distal position. These may indicate that some reducing environment, such as the glutathione cycle may promote the iron-induced injuries. The origins for the above facts were elucidated on the basis of the chemical points of view.

3. Structural Property of Active Species to Induce Renal Proximal Tubular Injuries by the Iron(III)-(nta) and its Derivatives

We have at first determined that crystal structures of several iron(III) compounds including (nta).[18,19] As shown in Figure 2, Fe(III)-(nta) complex is of a dimeric structure with oxo- and carbonato-bridge. The bent Fe-O-Fe core is consistent with the unique absorption spectra shown in Figure 3.[21] The structure of the Fe(III)-(edda) complex should be similar to that of the (nta)-
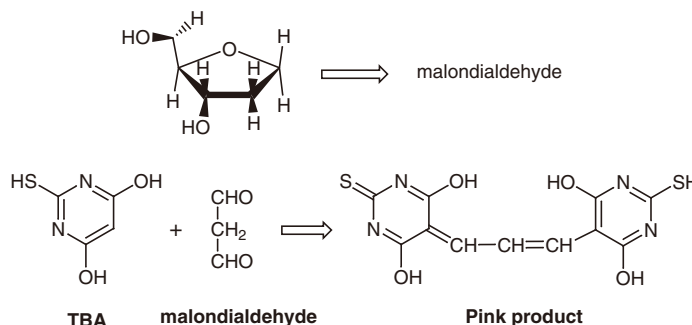
Scheme 1.
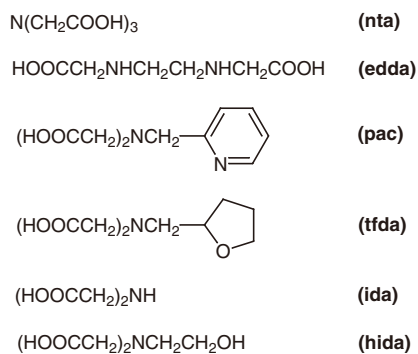
Figure 1. Several chelates cited in this review.

Table 1. Effects of iron chelates on renal tubular injuries.

	(+, active; −, inactive)		
Iron chelates	pH 6.2	pH 7.2	pH 8.2
Fe-(nta)	+	+	+
Fe-edda	+	+	+
Fe-ida	+	+	−
Fe-edta	−	−	−
Fe-pac	−	−	−
Fe-hida	−	−	−

chelate based on the absorption spectrum of this compound. It should be noted here that although the crystal structure of the Fe(III)-(pac) complex is of a dimeric structure (Figure 4) similar to that of the (nta)-compound, tubular injuries by the Fe(III)-(pac) compound is negligible (see Table 1) and the Fe(III)-(pac) compound does not induce the renal carcinoma, and that tubular injuries by the Fe(III)-(edda) compound is much less than that by the (nta)-complex (see Table 1, and Figure 5).[17,21]

When we compare the chemical properties of the three iron(III) compounds including (nta), (edda) and (pac) ligands, several differences are detected; at first, the activity for TBARS formation (see Scheme 1; see absorbance at 532 nm) in the presence of ribose and hydrogen peroxide is remarkable for the Fe(III)-(nta) complex, but the effect by the Fe(III)-(pac) compound is negligible, and that by the Fe(III)-(edda) is much weaker than that of the (nta)-chelate (see Figure 6).[20]

Crystal structural data of the two compounds, (nta) and (pac) (see Table 2) have revealed that the dimeric structure of the (pac) complex is stronger than that of the corresponding (nta)-compound, because the distances of both the Fe-O (oxo oxygen) and Fe-O (carbonato ion) distances are shorter in the (pac)-compound than those in the (nta)-compound. Based on these facts including absorption and ESR spectral data, it seems quite reasonable to conclude that the active species which decomposes ribose to give TBARS should be a $(\mu\text{-}\eta^1\text{:}\eta^1)$-peroxodiiron(III)-(nta) species shown in Scheme 2;[18,20] the high reactivity of the $(\mu\text{-}\eta^1\text{:}\eta^1)$-peroxodiiron(III) species similar to that of singlet oxygen $(^1\Delta_g)$ has been confirmed by our studies,[22,23] and the negligible activity by the (pac)-compound can be attributed to the inertness of the carbonato chelate, preventing the formation of a $(\mu\text{-}\eta^1\text{:}\eta^1)$-peroxodiiron(III) species even in the presence of hydrogen peroxide. In the case of the (edda)-compound, the carbonato ion in the dimeric unit is readily replaced by the hydrogen peroxide, leading to the formation of a dimeric species with a linear Fe-O-Fe core and also formation of a monomeric species;[20,24] this may explain the much smaller activity by Fe(III)-(edda)-compound for the formation of TBARS.
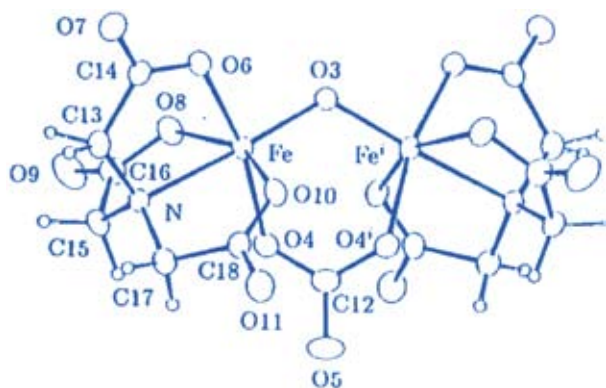
Figure 2. Crystal structure of $[Fe_2O(nta)_2(CO_3)]^{4-}$ ion.
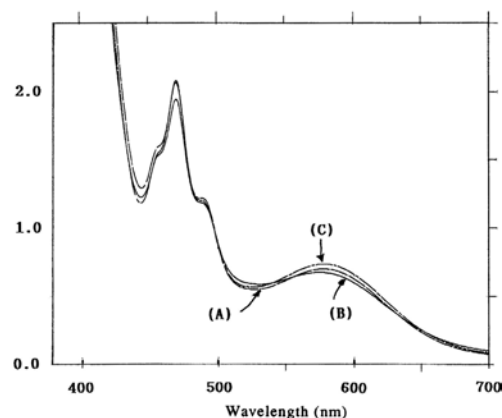
Figure 3. Spectral data of Fe(III)-(nta) chelate (in water, pH 7.0). (A) Fe(III)-(nta) solution ($[Fe_3^+]$ = 1/60 M). (B) Fe(III)-(nta) solution containing H_2O_2, measured immediately after addition of H_2O_2 ($[Fe_3^+]$ = $[H_2O_2]$ = 1/60 M). (C) measured 15 min. after addition of H_2O_2.

Table 2. Bond distances (Å) of the iron(III) chelates.[18-20]

	Fe-nta	Fe-pac
Fe-Fe	3.188	3.186
Fe-N	2.246	2.235
Fe-O(oxo)	1.83	1.8
Fe-O4(CO_3)	2.005	1.984
Fe-O6	2.025	2.061
Fe-O8	2.02	2.02
Fe-O10	2.082	
Fe-N(py)		2.166
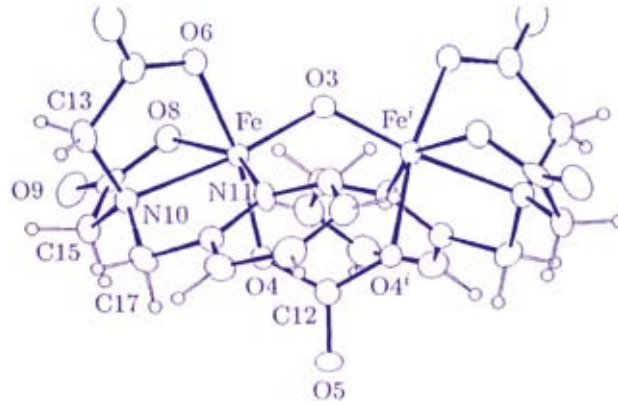
Figure 4. Crystal structure of $[Fe_2O(pac)_2(CO_3)]_2^-$ ion.
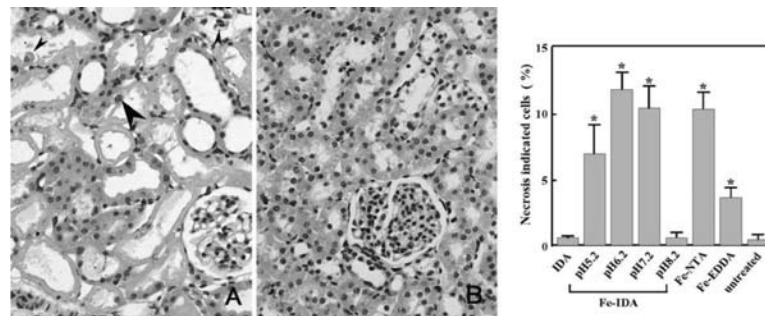
Figure 5. Proximal tubules necrosis in rat kidneys 6 h after injection of (A) Fe(III)-IDA at pH 6.2, (B) Fe(III)-IDA at pH 8.2. Hematoxylin and eosin staining (magnification, 100). Proximal tubular cells were specifically destroyed by Fe(III)-IDA at pH 5.2, 6.2, and 7.2. Effects of Fe(III)-IDA at pH 8.2 were not observed. Patchy degeneration of the proximal tubular epithelium with pyknotic nuclei (small arrowheads). Regenerative cells are large and irregularly shaped with prominent nucleoli (large arrowheads).[17]
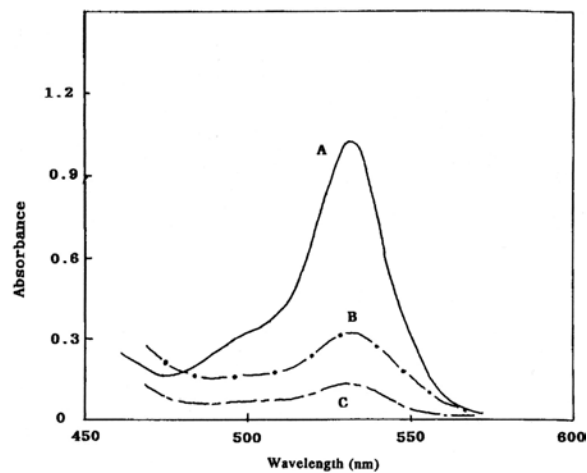
Figure 6. Absorption spectra of the solution containing iron(III) complex, ribose and hydrogen peroxide, treated by TBA(=2-thiobarbituric acid). A: Fe(III)-(nta), B: Fe(III)-(edda), C: Fe(III)-(pac).
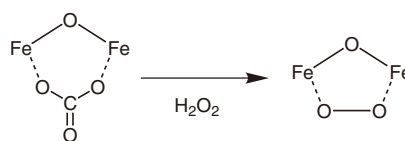
Scheme 2. Formation of $(\mu\text{-}\eta^1\text{:}\eta^1)$-peroxodiiron(III)-(nta).

4. Proximal Tubular Injuries by the Fe(III)-(ida) Compound

When the Fe(III)-(ida) was isolated as an orange crystal from the solution containing ferric chloride and iminodiacetic acid (hereafter we would like to use the R = [ida]/[Fe^{3+}] in the preparation of the iron(III) solution; generally R = 4 was employed) at pH~7.0 under 25 °C, it consists of a dimeric unit with a linear Fe-O-Fe bridge, as illustrated in Figure 7.[17] Two iminodiacetic acid molecules are coordinated to one iron(III) ion; one acts as a tridentate ligand, and another, as a bidentate ligand (in the discussion on the crystal structure, R' = [ida]/[Fe^{3+}] was used to characterize the crystal structure of the compound ; R' = 2 for the complex illustrated in Figure 7 and it should be noted here that R' and R are different from each other).

The TBARS formation detected in the solution containing hydrogen peroxide, iron(III) ion and iminodiacetic acid with the various ratio R = 1.2~3.2, are shown in Figure 9.[25] The TBARS formation is negligible when R = 3.2 in the pH range 7~8.0, and is not dependent on the pH (7~8) of the solutions when R = 1.2. As the activation of the peroxide ion does not occur when the peroxide ion cannot coordinate to an iron(III) ion, almost all the iron(III) species in the solution of R = 3.2 with pH 7~8 can be considered to be a dimeric structure with R' = 2

illustrated in Figure 7. Thus, it seems reasonable to speculate that there are oxo-bridged dimeric iron(III) species with R' = 1 species, as demonstrated in Figure 8, in the solutions of R = 1.2, which is consistent with the mass spectral data of these iron(III) compound solutions.

These demonstrate that there is an equilibrium in the solutions of Fe(III)-(ida) as shown in Eq. 1.

When the Fe(III)-(ida) solution with R = 4 was heated to above 40°C, brown precipitates, maybe Fe(OH)$_3$, occurred. This may demonstrate that the Fe-O-Fe structure with R' = 2 species (Figure 7) is less stable than the corresponding R' = 1 species (Figure 8), and this has been confirmed by the crystal structural data; the Fe-O distances are longer in the Fe(III)-(ida) species with R' = 2 (Figure 7) than those of the corresponding compounds where the iron(III) ions have weaker ligands such as chloride ions.[26]

In the rats administered with the iron(III)-(ida) solution with R = 4, it is reasonable to consider that concentrations of the iron(III) ion, (ida), and carbonato ion, are diluted with time. As the equilibrium of the Eq. 1 is dependent on the concentration of the (ida), the concentration of the species with R' = 2 may decrease and that of the R' = 1 may increase with time. In the beginning stage of the administration, since the temperature of the Fe(III)-(ida) solution was raised above 35 °C, and thus we
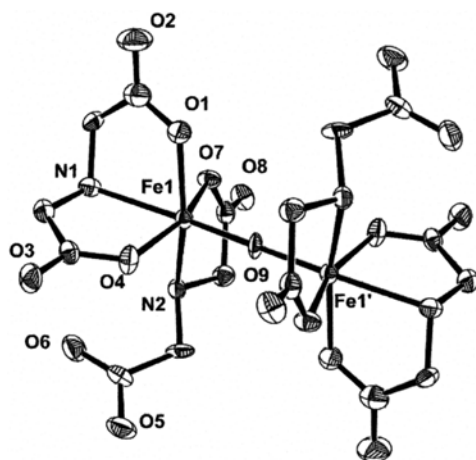
Figure 7. Crystal structure of [Fe$_2$O(ida)$_4$]$^{4-}$ ion.
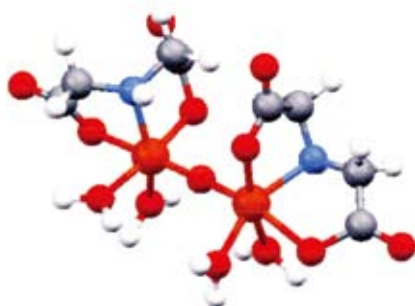
Figure 8. Optimized structure of [Fe$_2$O(ida)$_2$(H$_2$O)$_4$] based on the PM5 method.

can assume that $Fe(OH)_3$ may form, which is consistent with the report by Mizuno; this may explain the fact that tubular injury by the administration of the Fe(III)-(ida) solution with pH 8.0 and R = 4 is negligible.[17] In the cases of the solution of the R = 1.2 with pH 7~8, the iron(III) ions in the chelate are available to interact with the hydrogen peroxide, because the main species present in the solution should be that with R' = 1 in Figure 8.

In order to confirm the validity of the above discussion, we have investigated the hydrogen peroxide activation by several iron(III) compounds such as (Hedta)[27] and (epy);[26] the crystal structure of the latter compound being illustrated in Figure

10. In the binuclear iron(III) with (Hedta), iron(III) ions are all surrounded by the ligand atoms. On the other hand, in the case of Fe(III)-(epy), two positions are coordinated by the two chloride ions, which may be displaced by the water molecules in the aqueous solution and this situation may provide a chance for peroxide ion to coordinate to an iron(III) ion. In fact, binuclear iron(III) complex, $[Fe_2O(epy)_2Cl_2]^{2+}$ shows high activity for oxygenation of alkane in the presence of hydrogen peroxide,[26] but the tissue injury by the (Hedta) complex is negligible, as shown in our experiment.[17]
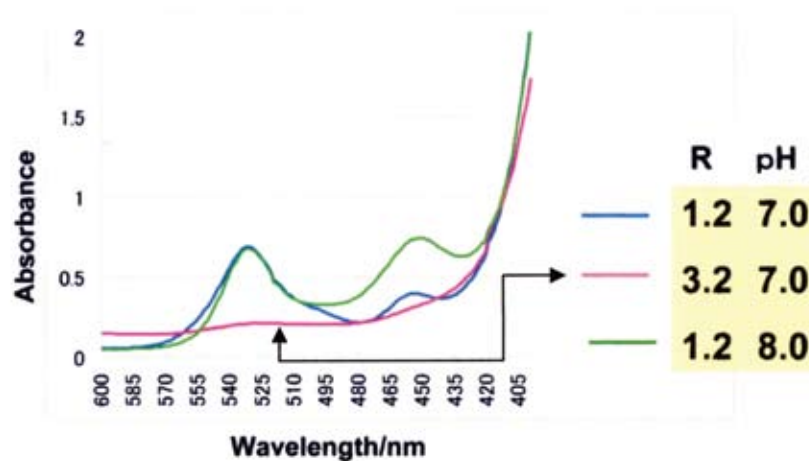
Figure 9. Absorption spectra of the solution containing iron(III)-(ida) complex, ribose and hydrogen peroxide, treated by TBA(= 2-thiobarbituric acid) blue; R = 1.2, pH 7.0, pink; R = 3.2, pH 7.0, green; R = 1.2, pH 8.0.

$$Fe_2O(ida)_4{}^{4-} \longleftrightarrow Fe_2O(ida)_2(H_2O)_4 + 2\ (ida)^- \qquad (Eq.\ 1)$$

(epy)

(Hedta)
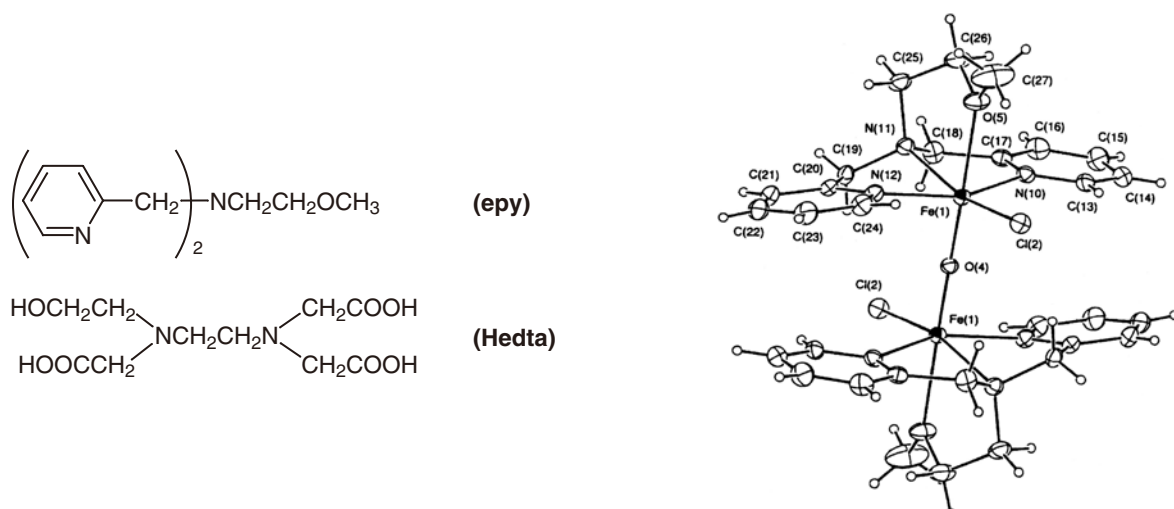
Figure 10. Crystal structure of $[Fe_2O(epy)_2Cl_2]^{2+}$ ion.

5. Why the Tissue Damage Occurs Only in the Vicinity of Renal Proximal Tubules?

As stated before, the proximal tubules necrosis and renal carcinoma induced by iron(III)-(nta) and other related compounds are observed mainly in the renal proximal tubules, but injury was not observed in the distal position, although many iron(III) ions are present in that position.[17] It should be noted here that the glutathione cycle is highly active in the renal proximal position,[28] and this may demonstrate that the glutathione cycle may promote the iron(III)-induced injuries.

At first, we will consider the interaction between an iron(III) chelate and the protein. It is generally recognized that transferrin carries an iron(III) ion in the human body, and it receives an iron ion from ferritin. However, the detailed mechanism of iron ion transfer from ferritin to transferrin remains unclear at present. In order to clarify the mechanism of iron-ion transfer, we have investigated the interactions between several iron(III) chelates and apo-transferrin. The formation of holo-transferrin was checked by ESR spectra, absorption spectra, and capillary electrophoresis; in the latter method the shift of the peak position in the CE diagram to longer separation time is diagnostic for the formation of the holo-transferrin.[24]

From the results, it has become apparent that the transfer of the iron(III) ion from the iron(III)-chelates to apo-transferrin is highly dependent on the structure of the iron(III)-chelates;[24] strange to say, its trend is very similar to those in the Table 1. For example, in the alkoxo-bridged binuclear iron(III) complexes, $Fe_2(hida)_2(H_2O)_2$[29] and $Fe_2(HPTP)Cl_4$, the iron(III) ions of only the latter complex are readily transferred to apo-transferrin, but those of the former complex do not.

Our results have lead to the conclusion that interaction between the two iron(III) ions and the surface of the protein at the two points, as illustrated in Scheme 3, is necessary for the facile transfer of the iron(III) ions. In the case of $Fe_2(hida)_2(H_2O)_2$ two iron(III) ions cannot interact with the surface at the two points similar manner to described in Scheme 3 because of the steric hindrance of this complex (Figure 11); on the other hand such two-point interaction is possible for the $Fe_2(HPTP)Cl_4$ complex,[30] because the four chloride ions are labile in the aqueous solution (see Figure 12).

In 1973, Bates et al. reported that iron(III) ions of the Fe(III)-(nta) are readily transferred to apo-transferrin,[31] and this may be explained as follows; as mentioned before the carbonato ion of the binuclear complex, $Fe_2O(nta)_2(CO_3)$ is labile, and it may readily dissociate from the complex in the reaction of the oxygen or nitrogen atoms present on the surface of apo-transferrin and thus the two-point interaction between two iron(III) ions and apo-transferrin may readily occur (see Scheme 3).

When green crystals of Fe(III)-(edda) complex once isolated were mixed with apo-transferrin in buffer solution, the transfer of the iron(III) ions to apo-transferrin is largely reduced compared with that of Fe(III)-(nta) chelate.[24] This may be elucidated as follows; the color of the buffer solution containing green crystalline Fe(III)-(edda) complex is light yellow, illustrating that the concentration of the green iron(III) species with the bent Fe-O-Fe unit is greatly decreased, and dissociation of the dimeric compounds to monomeric species was confirmed by the ESR spectrometry. This should be main reason for the fact that the transfer of the iron(III) ions to apo-transferrin is largely reduced. The dissociation of a dimeric species to a monomeric one may proceed when the green Fe(III)-(edda) solution is administrated into rat, because the concentrations of the ligand and carbonato ions decrease with time. This explains the lower effect for tissue injury by the administration of Fe(III)-(edda) solution as demonstrated in Table 1.
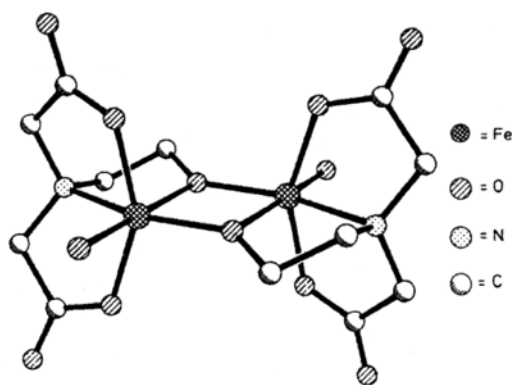
Figure 11. Crystal structure of $[Fe_2(hida)_2(H_2O)_2]$.
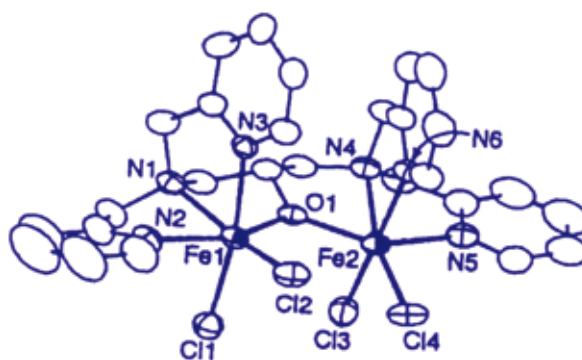
Figure 12. Crystal structure of $[Fe_2(HPTP)(Cl)_4]^+$ ion.
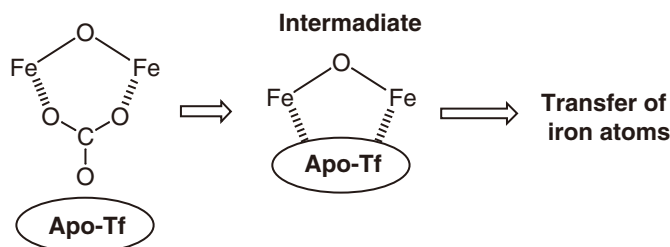
Scheme 3.

Next, we will consider the interaction between binuclear iron(III) chelates and the glutathione cycle. According to the discussions described above, some iron(III) chelates may interact with the glutathione cycle through the two-point interaction. It should be remembered here that some binuclear iron(III) compounds exhibit very unique reactivity towards reducing agents in the presence of oxygen. For example, the binuclear iron(III) complex with H(HPTB), Fe_2(HPTB)(OH)$(NO_3)_2$ exhibits high activity for oxygenation of linolenic acid in the presence of oxygen, and two-electron transfer reaction to oxygen (formation of hydrogen peroxide) from TMPD (*N,N,N',N'*- tetramethyl-*p*-phenylenediamine).[32,33] This has been elucidated on the assumption that a binuclear iron(III)-oxygen intermediate formation is promoted through the interaction with reducing agent, such as linolenic acid or TMPD (Scheme 4).[33,34]

The importance of two-point interaction between binuclear two iron(III) ions and oxygen is again emphasized! Although the detailed mechanism of the above reaction remains unclear (see Chapter 7), it is reasonable to assume that iron(III)-chelate which can interact with apo-transferrin at the two points can interact with oxygen under the presence of reducing agent. In fact, the binuclear iron(III) complex, Fe_2(HPTP)(OH)$(NO_3)_2$, can oxygenate the linolenic acid in the presence of oxygen, and exhibit high activity for tissue injury when administered in rat. As it has been exemplified that the binuclear iron(III) complex, Fe_2(HPTP)(OH)$(NO_3)_2$ shows high activity for formation of hydrogen peroxide in the presence of TMPD,[33] it seems reasonable to speculate that the high tissue damage by Fe_2(HPTP)(OH)$(NO_3)_2$ should be due to the formation of a peroxide adduct of the binuclear compound in the reaction of the glutathione cycle in the presence of oxygen.[24]
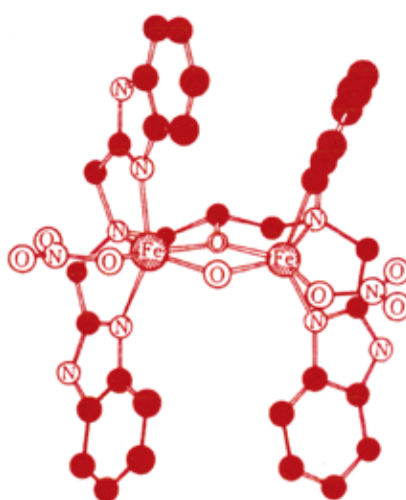
Structure of [Fe_2(HPTB)(OH)$(NO_3)_2$]$^{2+}$ ion.

H(HPTP)

H(HPTB)
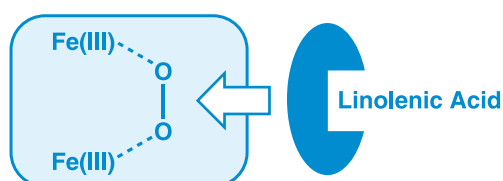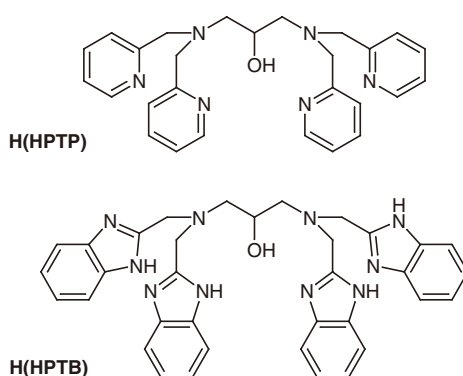
Scheme 4. Assumed structure of intermediate compound containing binuclear iron(III) complex, oxygen and linolenic acid.
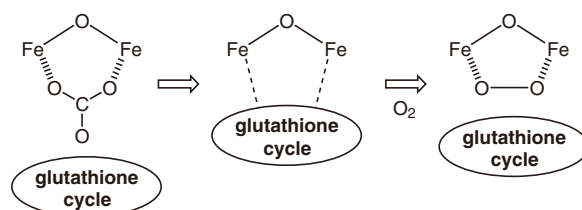
Scheme 5. Assumed scheme for Fe(III)-(nta)-peroxide adduct formation of in the reaction mixture of Fe(III)-(nta) chelate and glutathione cycle.

Based on the above discussion, the tissue damage and renal carcinoma by the Fe(III)-(nta) chelate may be explained as follows (see Scheme 5);[24] when binuclear Fe(III)-(nta) compound reacts with the glutathione cycle, the carbonato ions dissociate from the compound, leading to the interaction between two iron(III) atoms and the protein. At this stage, when oxygen is present, formation of peroxide ion may be accelerated through the interaction between the glutathione cycle, and the formed peroxide adduct of the binuclear Fe(III)-(nta) complex shows high oxidative reactivity[22,23] towards the proteins, leading to the tissue injuries and renal carcinoma. Thus, the tissue damage and renal carcinoma occur only in the renal proximal tubules where glutathione cycles are highly operating.[28]

Our conclusion on the active species to induce tissue damage and renal carcinoma (see Scheme 5) can explain comprehensively all the results demonstrated in Table 1 and others not cited in the table. In many previous papers, the role of the hydroxyl radical in inducing the tissue damage and renal carcinoma has been frequently pointed out,[15] but this cannot explain the lower activity in the tissue damage by the Fe(III)-(edda) chelate and the difference in the tissue damage between the two alkoxo-bridged binuclear iron(III) complexes, $Fe_2(hida)_2(H_2O)_2$ and $Fe_2(HPTP)Cl_4$, and also between Fe(III)-(nta) and Fe(III)-(pac) chelates.

6. Models of NTBI and the Origin of Toxicity

Abnormally high levels of iron in the brain have been demonstrated in a number of neurodegenerative disorders, including Parkinson's disease and Alzheimer's disease (AD), and oxidative stress closely related with the increased iron levels in the brain and possibly also from defects in antioxidant defense mechanisms are widely believed to be associated with neuronal death in these diseases.[35-40] But a key question – why do iron levels increase abnormally in some regions of the brain? – has not been answered. The abnormalities in iron ion metabolism have been pointed out to be one of the important origins inducing the iron ion accumulation, and the abnormalities in iron ion metabolism may occur due to accumulation of large excesses of Al and Mn ions in the brain.[3]

We have found that deposition of iron(III) hydroxide occurs readily on the aggregates of amyloid beta-peptide (1-40) induced by zinc(II) chloride in the solution containing iron(III) compounds with (nta), (edda), and other amino acid derivatives;[41] the deposition of iron(III) hydroxide may proceed *via* the coordination of nitrogen and oxygen atoms of the amino acid residues of the amyloid beta-peptide (1-40) to the iron(III) atom, similar to that illustrated in Scheme 4. These facts are implying that iron(III) compounds with amino acids or peptides in plasma may be an intrinsic iron(III)-ion carrier to induce the high level accumulation of iron(III) ions in the amyloid deposits, and thus it seems quite reasonable to assume that several

$$2Fe(epy)Cl_2 + H_2O \longrightarrow Fe_2O(epy)_2Cl_2$$

(Eq. 2)

$$2Fe(dpal)Cl_2 + H_2O_2 + e^- + H_2O \longrightarrow 2Fe_2O_2(dpal)_2$$
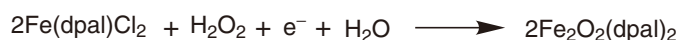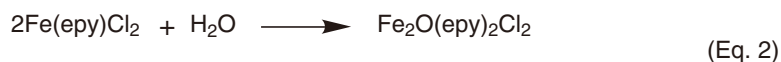
(One of the two oxo-atoms is derived from hydrogen peroxide)

iron(III) compounds with amino acids or peptides in plasma are possible candidate for NTBI models.

Recently it has been suggested that the toxicity of Aβ and other amyloidogenic proteins lies not in the insoluble fibrils that aggregate but rather in the soluble oligomeric intermediates, indicating that the soluble oligomers may be more important pathologically than are the fibrillar deposits.[42,43] The origin of the high toxicity of the soluble oligomeric intermediates should be due to the iron(III) species bound in the oligomers, which may contain a dimeric iron(III) species or those with oxo-bridges; the soluble iron(III) species in the oligomers readily turns to a dimeric species with oxo-bridge in the presence of hydrogen peroxide, as exemplified *in vitro* (see Eq. 2).[26,44]

These dimeric iron(III) compounds with an oxo-bridge in the oligomeric intermediates should be an intrinsic active species in the oxidative stress observed for neurodegenerative disorders, including Parkinson's disease and Alzheimer's disease (AD). Based on the present results and the discussion, we would like to propose that the formation of insoluble amyloid plaques including iron(III) ions promoted by the zinc(II) ions may be one of the important methods to protect the oxidative stress by soluble oligomeric iron(III) compounds with amino acids or peptides (NTBI) *in vivo*.[41]

7. Theoretical Background in Iron-Oxygen Interaction and Activation of Oxygen Molecule

The electronic configuration of the oxygen atom is $1s^2 2s^2 2p^4$. When two O atoms combine to form O_2, the same orbital types combine if they are of equal or approximately equal energy. Thus, the 1s, 2s, $2p_x$, $2p_y$, and $2p_z$ on one oxygen combine with the similar orbitals on the other oxygen to give, in each case, two MO's. The five AO's on each atom give rise to ten MO's in the molecule.[46]

Since the electrons will occupy the orbitals in the order of increasing energy, we must arrange our MO's in an energy sequence so that we can place our sixteen electrons properly. One of the most instructive ways to do this is by means of the molecular orbital energy diagram method. In the oxygen molecule we have the combination of both 1s and 2s orbitals to give four σ type orbitals, two bonding and two antibonding, each of them occupied by two electrons. Because the 1s electrons are not valence electrons, we usually pay little heed to them. The combination of the 2s orbitals does not result in any net bonding (see Scheme 6).

The three atomic p orbital levels in the isolated atom are of equal energy (degenerate); but when we bring one atom into the field of the other, the p_z orbitals pointing toward the other atom start to interact to form a σ bond between the two atoms. The corresponding σ* orbitals are generated. These orbitals $\sigma_g(2p_z)$ and $\sigma_u^*(2p_z)$, are in fact σ molecular orbitals because they are
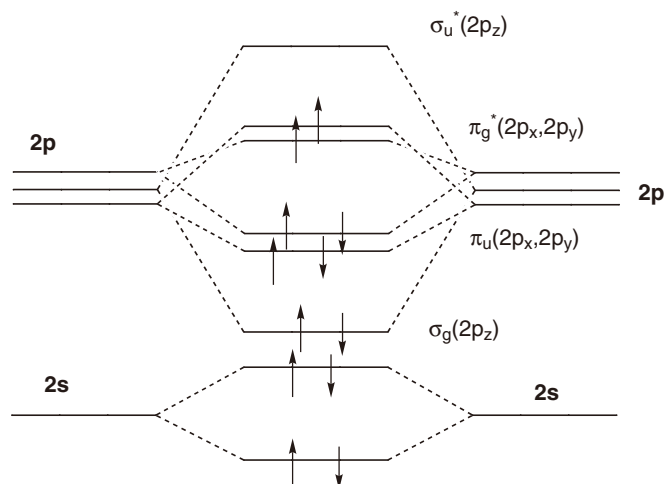
Scheme 6. MO scheme for O_2.

symmetric with respect to rotation around the internuclear axis (in this case, z-axis). The bonding interaction is quite large, and hence the splitting is also relatively large (see Scheme 6).

The p_x and p_y orbitals on each oxygen combine to each from a π set: $\pi_u(2\pi_u(2p_x)$, $\pi_g*(2p_x)$, $\pi_u(2p_y)$, $\pi_g*(2p_y)$. The p_x and p_y orbitals are perpendicular to each other. Now, if we refer to our MO energy diagram, we see that six electrons of 2p orbitals are referred to as valence electrons, that is these electrons occupy $\sigma_g(2p)$ and $\pi_u(2p)$. If we follow the principles used for the periodic classification, the two electrons must go separately into the $\pi_g*(2p_x)$ and $\pi_g*(2p_y)$ orbitals, with spin parallel (Hund's rule: see Figure 5 and Table 2). The two unpaired electrons in the π* orbitals give rise to the paramagnetic properties of molecular oxygen. The diradical character and accompanying paramagnetism of oxygen constitute its outstanding property.

The occupation of antibonding orbitals by one or more electrons cancels some of the bonding attraction between the atoms. In the O_2 example, we have two π bonding orbitals, each doubly occupied, and a σ bonding orbital, doubly occupied, or a total of three bonding orbitals. However, each of the two electrons in an antibonding orbital cancels the bonding effect of an electron in a bonding orbital, and so the net bonding in oxygen can be considered to result from a double bond. Evidence for the effect of occupation of the antibonding orbitals comes from bond distances. In the ground state, the bond distances between oxygen atoms is 1.207 A. However, when O_2 is ionized by loss of an electron from one of the π* antibonding orbitals, the resulting O_2^+ is 1.123 A, a considerable decrease, indicative of stronger bonding in the ion. The bond lengths of O_2^- (a radical anion) and O_2^{2-} are 1.28 and 1.49 A, respectively, confirming the fact that electrons have been added to antibonding orbitals.

It should be noted here that O-O bond of the peroxide ion is cleaved by acceptance of another one electron; this clearly demonstrates that triplet O_2 molecule does not react with the usual organic molecules which contains no unpaired electrons!

It is known from chemical studies that O_2 can be converted from its ground triplet state to a singlet state if energy is supplied, usually in the form of light in the presence of a photosensitizer. Two types of singlet oxygen are known (see Table 3) and of these $^1O_2(^1\Delta_g)$ is more interesting. Singlet state $^1O_2$ ($^1\Delta_g$) has a reactivity which is quite different from that of triplet O_2; for example, $^1O_2$ ($^1\Delta_g$) reacts very rapidly with alkenes at room temperature to give allylic peroxides or conjugated dienes to give cyclic peroxides (see Scheme 7).

7-1. Oxygen activation through Interaction with iron ion

Despite its greater reactivity, it is unlikely that singlet O_2 is involved in very many biological oxygenase reactions; the most persuasive argument against the involvement of singlet O_2 in biological reactions is that the lowest energy singlet state ($^1\Delta_g$) is 22 kcal/mole higher in energy than the ground state triplet, and it is not apparent how an enzyme could supply electronic energy of that magnitude. For this point, we have experimentally showed that the interaction between unpaired electrons of oxygen and a transition metal ion can change the triplet oxygen molecule to act as a singlet oxygen ($^1\Delta_g$), and this may be rationalized in the figure below.[46-49] In this case, the formation of the unoccupied antibonding orbital **b** is very important, which exhibits high affinity for the occupied orbitals of the organic compounds (electrophilicity).

However, the interaction between unpaired electrons of oxygen and a transition ion does not occur under the usual conditions; for example copper(II) ion has one unpaired electron, but its aqueous solution (solution of copper sulfate) exists stably, and does not react with oxygen in the air. This is

1,3-Addition(ene-reaction)

1,4-Addition(Endperoxide formation)
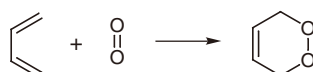
Scheme 7.

Table 3. Electronic configurations of singlet oxygen.

State	π*(2p$_x$)	π*(2p$_y$)	Energy
$^1\Sigma_g{}^+$	↑	↓	155 kJ (~13,000 cm^{-1})
$^1\Delta_g$	↑↓	—	92 kJ (~8,000 cm^{-1})
$^3\Sigma_g{}^-$	↑↓	↑	0 (ground state)

partly because of the fact that the d-orbital which contains one unpaired electron is covered by a water molecule, preventing the approach of oxygen to this orbital. Thus, in order to induce the interaction between unpaired electrons of oxygen and transition ion, other chemical compounds are necessary.

Possibly another chemical compound may be a reducing agent, because we can detect the interaction between unpaired electrons of oxygen and the transition ion under electrochemical measurements as shown in Figure 13 (the appearance of the additional CV peak indicated by the arrow has been attributed to the presence of the oxygen interacting with an unpaired electron of $V^{IV} = O$ ion).[50,51] The origin for this fact is not clear at present, but it seems to be reasonable to assume that the electronic energy of systems containing oxygen, transition ion and the electrode is lowered through interaction with the occupied orbitals of the electrode and unoccupied orbital **b**.

Thus, several reducing agents which interact with the unoccupied orbital **b** in Scheme 8 can promote the formation of an intermediate compound containing metal ion, oxygen, and reducing agent, and there are many reports to support that the oxygen in the intermediate can act as a singlet oxygen $^1O_2$ ($^1\Delta_g$).[32-34,46-49] The changed triplet oxygen can interact with several organic compounds, leading to the oxygenation of the linolenic acid according to the 1,3-diene reaction in Scheme 7. The intermediate described in Scheme 4 may be accelerated by the presence of linolenic acid or TMPD, and also the pterin may play an important role to give the intermediate containing tyrosine hydroxylase, oxygen, tyrosine, and pterin, leading to activation of the oxygen molecule to give dopa from tyrosine.[49]
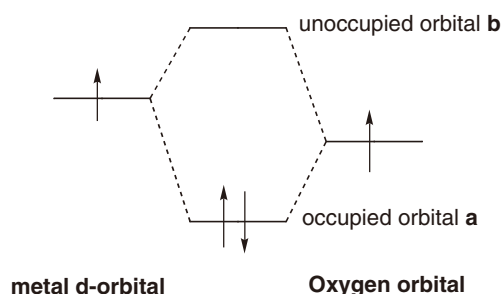
Scheme 8.
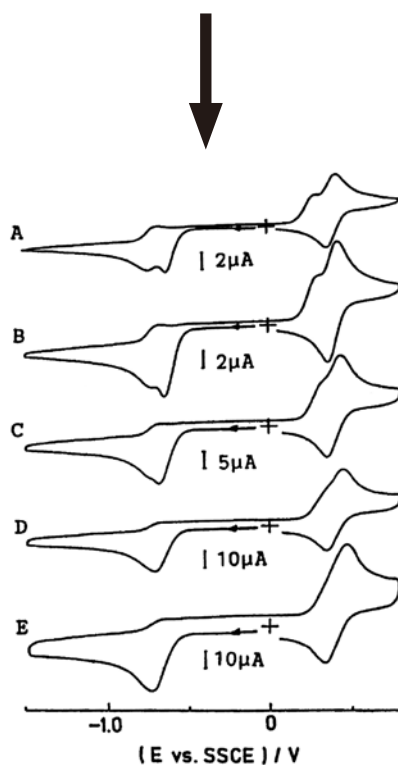
Figure 13.[50]   CV of oxygen molecule in the presence of [VO(salen)] (in DMSO, $[O_2]$ = 0.47 mM, [VO(salen)] = 1 mM, 25 °C). A: at scan speed 20 mV/s, B: 50 mM/s, C: 200 mV/s, D: 500 mV/s, E: 1000 mV/s.

7-2. Activation of Peroxide Ion by Iron(III) Ion

The high activity of the peroxide ion coordinated to the binuclear iron(III) compounds is also rationalized similarly to the above discussion. As stated before, the peroxide ion has no unpaired electron and two π^*-orbitals are doubly occupied, and thus under the usual conditions, this peroxide ion does not react with organic compounds. In the binuclear iron(III)-peroxide adduct with (μ-η^1:η^1)-configuration in Scheme 2, one of the two occupied π^*-orbitals interacts with the d-orbital derived from the magnetically interacting two iron(III) ions (see the d-orbital in Scheme 9 illustrated in the left side), which may be unoccupied. Then, an unoccupied orbital **b** (shown in Scheme 9) also forms in this process, and thus under this condition the peroxide ion coordinated to the two iron(III) ions operates as a singlet oxygen $^1O_2$ ($^1\Delta_g$),[22,23] which is confirmed by many experimental results.[52]

In the case of monomeric iron(III)-peroxide adduct, Fe(III)-OOH, the reactivity of the coordinated peroxide ion should highly depend on the spin-state of the iron(III) ion of the chelate. If the Fe(III) is of low-spin type, such as cytochrome P-450 where the d_{z^2}-orbital interacting with the peroxide ion is unoccupied, unoccupied orbital **b** also forms as demonstrated in Scheme 9. When the iron(III) ion is of high-spin-type, such situation as described in Scheme 9 does not occur, and the peroxide ion coordinated to the iron(III) ion may be inert. But, if there is another organic compound (substrate or spherical group) in the system, three-orbital interaction[53] may occur as illustrated in Scheme 10, leading to the formation of unoccupied orbital **b** in Scheme 10. In these cases the metal-peroxide adducts are highly dependent on the spherical organic groups surrounding the metal core.[3,54,55]

8. Summary

As demonstrated in Introduction, NTBI has been detected in the plasma of patients with thalassemia, hemochromatosis and other iron-overloading disorders, as well as in patients receiving chemotherapy, and NTBI has been thought to play an important role in iron induced cell damage with resultant peroxidation of cell membrane lipids and other biomolecules. According to our results described in this review, it is quite clear that the role of the Fenton reaction to give hydroxyl radical is negligible in the oxidative stress and the oxidative damages due

unoccupied orbital **b**

occupied orbital **a**

d-orbital   peroxide ion

Scheme 9.

unoccupied orbital **b**

orbital of organic compound

occupied orbital of peroxide

occupied orbital **a**

d-orbital
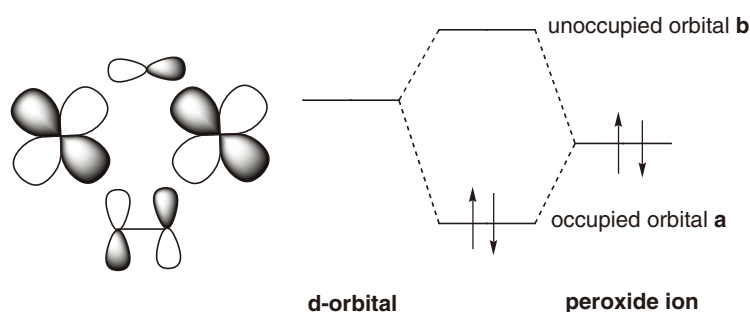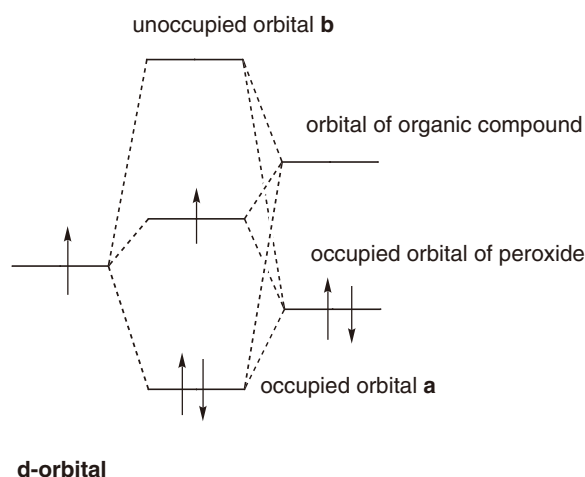
Scheme 10.

to a peroxide adduct of the binuclear iron(III) chelates should be a main contributor in the pathogenesis of cancer, cardiovascular disease, aging and other degenerative diseases. In addition to above we would like to point out that NTBI should be iron(III) chelates with amino acids or small peptides derived from the insoluble hemosiderin. Based on the our experimental results *in vitro*, we have reported new chelates which bind the iron ions in NTBI, but do not bind the iron(III) ions in transferrin, which may contribute to advances in iron overload therapies.[56-58]

References

1. J. M. McCord, *Nutrition Rev.* **1996**, *54*, 85.
2. E. Beutler, A. V. Hoffbrand, J. D. Cook, *Amer. Soc. Hematology* **2003**, 40.
3. Y. Nishida, *Med. Hypothesis Res.* **2004**, *1*, 227.
4. P. M. Harrison, P. Arosio, *Biochim. Biophys. Acta* **1996**, *1275*, 161.
5. N. D. Chasteen, P. M. Harrison, *J. Struc. Biology* **1999**, *126*, 182.
6. B. Dresow, D. Petersen, R. Fischer, P. Nielson, *Biometals* **2008**, *21*, 273.
7. R. Grosse, U. Lund, V. Caruso, R. Fischer, G. E. Janka, C. Magnano, R. Engelhardt, M. Dürken, P. Nielsen, *Ann. N. Y. Acad. Sci.* **2005**, *1054*, 429.
8. B. P. Esposito, W. Breuer, P. Sirankapracha, P. Pootrakul, C. Hershko, Z. I. Cabantchik, *Blood* **2003**, *102*, 2670.
9. Z. I. Cabantchik, W. Breuer, G. Zanninelli, P. Cianciulli, *Best Pract Res. Clin. Haematol.* **2005**, *18*, 277.
10. D. J. R. Lane, A. Lawen, *J. Biol. Chem.* **2008**, *283*, 12701.
11. S. Okada, O. Midorikawa, *Jpn. Arch. Intern. Med.* **1982**, *29*, 485.
12. J.-L. Li, S. Okada, S. Hamazaki, Y. Ebina, and O. Midorikawa, *Cancer Res.* **1987**, *47*, 1867.
13. S. Toyokuni, J. L. Sagripanti, *Carcinogenesis* **1993**, *14*, 223.
14. S. Ansah, M. Iqbal, M. Athar, *Carcinogenesis* **1999**, *20*, 599.
15. B.Halliwell, J. M. C. Gutteridge, in *Free Radicals in Biology and Medicine,* Oxford University Press, **1985**.
16. T. Kawabata, Y. Ma, I. Yamador, S. Okada, *Carcinogenesis* **1997**, *18*, 1389.
17. R. Mizuno, T. Kawabata, Y. Sutoh, Y. Nishida, S. Okada, *Biometals* **2006**, *19*, 675.
18. Y. Nishida, A. Goto, T. Akamatsu, S. Ohba, T. Fujita, T. Tokii, S. Okada, *Chem. Lett.* **1994**, 641.
19. T. Fujita, S. Ohba, Y. Nishida, A. Goto, T. Tokii, *Acta Cryst. Sect. C* **1994**, *50*, 544.
20. Y. Nishida, S. Ito, *Polyhedron* **1995**, *14*, 2301.
21. M. Liu and S. Okada, *Carcinogenesis,* **1994**, *15*, 2817.
22. Y. Nishida, M. Takeuchi, *Z. Naturforsch. B* **1987**, *42*, 52.
23. S. Nishino, H. Hosomi, S. Ohba, H. Matsushima, T. Tokii, Y. Nishida, *J. Chem. Soc. Dalton Trans.* **1999**, 1509.
24. Y. Nishida, Y. Itoh, T. Satoh, *Z. Naturforsch. C* **2007**, *62*, 608.
25. Y. Sutoh, Y. Okawamukai, Y. Nishida, in press.
26. S. Ito, T. Okuno, H. Itoh, S. Ohba, H. Matsushima, T. Tokii, Y. Nishida, *Z. Naturforsch. B* **1997**, *52*, 719.
27. S. J. Lippard, H. J. Schugar, C. Walling, *Inorg. Chem.* **1967**, *6*, 1825.
28. S. Okada, Y. Minamiyama, S. Hamazaki, S. Toyokuni, A. Sotomatsu, *Arch. Biochem. Biophys.* **1993**, *301*, 138.
29. S. L. Heath, A. K. Powell, *Angew. Chem., Int. Ed. Engl.* **1992**, *31*, 191.
30. S. Nishino, M. Kunita, T. Kobayashi, H. Matsushima, T. Tokii, Y. Nishida, *Z. Naturforsch. B* **1999**, *54*, 1272.
31. G. W. Bates, M. R. Schlabach, *J. Biol. Chem.* **1973**, *248*, 3228.
32. Y. Nishida, K. Yamada, *J. Chem. Soc. Dalton Trans.* **1990**, 3639.
33. Y. Nishida, M. Takeuchi, H. Shimo, S. Kida, *Inorg. Chim. Acta* **1985**, *96*, 115.
34. Y. Nishida, M. Nasu, T. Akamatsu, *J. Chem. Soc. Chem. Commun.* **1992**, 93.
35. Y. Nishida, in *Inorganic-Biochemical Perspective of Sporadic Prion Diseases,* CIN Press, **2006**.

36. K. J. Thompson, S. Shoham, J. R. Connor, *Brain Res. Bull.* **2001**, *55*, 155.
37. P. Aisen, C. Enns, M. Wessling-Resnick, *Int. J. Biochem. Cell Biol.* **2001**, *33*, 940.
38. R. Liu, W. Liu, S. R. Doctrow, M. Baudry, *J. Neurochemistry* **2003**, *85*, 492.
39. M. Stefani, C. M. Dobson, *J. Mol. Chem.* **2003**, *81*, 678.
40. A. I. Bush, *Trends Neuroscience* **2003**, *26*, 207.
41. Y. Okawamukai, Y. Sutoh, Y. Nishida, *Synth. React. Inorg. Metal-Org. Nano-Metal Chem.* **2006**, *36*, 373.
42. R. Kayed, E. Head, J. L. Thompson, T. M. McIntire, S. C. Milton, C. W. Cotman, C. G. Glabe *Science* **2003**, *300*, 486.
43. W. L. Klein, W. B. Stine Jr., D. B. Teplow, *Neurobiol. Aging* **2004**, *25*, 569.
44. Y. Sutoh, Y. Okawamukai, S. Nishino, Y. Nishida, *Z. Naturforsch. C* **2006**, *61*, 149.
45. M. Orchin, H. H. Jaffe, in *SYMMETRY, ORBITALS AND SPECTRA*, John Wiley Sons, Inc, New York, **1971**.
46. Y. Nishida, T. Fujimoto, N. Tanaka, *Chem. Lett.* **1992**, 1291.
47. Y. Nishida, N. Tanaka, M. Okazaki, *Polyhedron* **1994**, *13*, 2245.
48. Y. Nishida, N. Tanaka, *J. Chem. Soc. Dalton Trans.* **1994**, 2805.
49. Y. Nishida, *Z. Naturforsch. C* **2001**, *56*, 865.
50. Y. Nishida, I. Watanabe, S. Takahashi, T. Akamatsu, A. Yamazaki, M. Sakamoto, *Polyhedron* **1994**, *13*, 2205.
51. Y. Nishida, N. Tanaka, A. Yamazaki, T. Tokii, N. Hashimoto, K. Ide, K. Iwasawa, *Inorg. Chem.* **1995**, *34*, 3616.
52. M. S. Chen, M. C. White, *Science* **2007**, *318*, 783.
53. R. S. Mulliken, W. B. Person, *in Molecular Complexes,* Wiley-Interscience, New York, **1969**.
54. S. Nishino, T. Kobayashi, M. Kunita, S. Ito, Y. Nishida, *Z. Naturforsch. C* **1999**, *54*, 94.
55. Y. Nishida, S. Nishino, *Polyhedron* **2003**, *22*, 293.
56. G. J. Kontoghiorghes, E. Eracleous, C. Economides, A. Kolnagou, *Current Med. Chem.* **2005**, *12*, 2663
57. A. El-Beshlawy, C. Manz, M. Naja, M. Eltagui, C. Tarabishi, I. Youssry, H. Sobh, M. Hamdy, I. Sharaf, A. Mostafa, O. Shaker, A. V. Hoffbrand, A. Taher, *Ann. Hematol.* **2008**, *87*, 545.
58. A. Kattamis, *Ann. N. Y. Acad. Sci.* **2005**, *1054*, 175.

Introduction of the author :

Yuzo Nishida*   Professor, Faculty of Science, Yamagata University

*Present address: Medical Research Institute, Kanazawa Medical University, 1-1 Daigaku, Uchinada, Kahoku, Ishikawa, 920-0261 Japan.

Yuzo Nishida received his Ph.D. from Kyushu University. He joined the Faculty of Science, Kyushu University as an assistant professor in 1969. He was promoted an associate professor at the Faculty of Science, Yamagata University in 1987, a professor at the Faculty of Science, Yamagata University in 1991, a professor at the Institute for Molecular Science in 1998, a professor at the Faculty of Science, Yamagata University in 2000. He has been a visiting professor at the Medical Research Institute, Kanazawa Medical University since 2009.
[Specialties] Coodination chemistry, Biological inorganic chemistry, Brain disease chemistry.